



Simulation of low-cycle fatigue residual stress in DP600 steel laser-welded structure

Miaoran Liu, Afia Kouadri-Henni, Benoit Malard

► To cite this version:

Miaoran Liu, Afia Kouadri-Henni, Benoit Malard. Simulation of low-cycle fatigue residual stress in DP600 steel laser-welded structure. ICRS 11 - The 11th International Conference of Residual Stresses, IJL; SF2M, Mar 2022, Nancy, France. hal-04227288

HAL Id: hal-04227288

<https://hal.univ-lorraine.fr/hal-04227288>

Submitted on 3 Oct 2023

HAL is a multi-disciplinary open access archive for the deposit and dissemination of scientific research documents, whether they are published or not. The documents may come from teaching and research institutions in France or abroad, or from public or private research centers.

L'archive ouverte pluridisciplinaire **HAL**, est destinée au dépôt et à la diffusion de documents scientifiques de niveau recherche, publiés ou non, émanant des établissements d'enseignement et de recherche français ou étrangers, des laboratoires publics ou privés.

SIMULATION OF LOW-CYCLE FATIGUE RESIDUAL STRESS IN DP600 STEEL LASER-WELDED STRUCTURE

Miaoran LIU^{a, b}, Afia KOUADRI-HENNI^{a, b, *}, Benoit MALARD^c

^a*INSA Rennes, 20 avenue des Buttes de Coësmes, 35708, Rennes, France*

^b*Laboratory of Digital Sciences of Nantes (LS2N), Team ROMAS, UMR CNRS 6004, 1 rue de la Noë, 44300, Nantes, France*

^c*CIRIMAT, Université de Toulouse, CNRS, INPT, UPS, 4 Allée Emilie Monso 31030 Toulouse, France*

ABSTRACT

With the Abaqus finite element method, the residual stress of DP600 steel after laser welding and low-cycle fatigue is simulated. Due to the large temperature gradient during laser welding and the cyclic loading during low-cycle fatigue, the material produces plastic deformation and strain hardening, in which strain is one of the main parameters affecting strain hardening. This paper first establishes plastic material constitutive models to simulate the laser welding residual stress. Then, low-cycle fatigue residual stress is simulated by the combined hardening models. Finally, the variability of residual stress is analyzed. The results show that residual stress is redistributed and relaxes after low-cycle fatigue. Furthermore, the simulation results are verified by experimental data.

Keywords: Finite element method; Residual stress; Low-cycle fatigue; Laser welding.

1. Introduction

Modern welding technology first appeared at the end of the 19th century. With the rapid development of welding technology, it can be divided into laser welding, arc welding, and electron beam welding according to different heat sources. Laser welding is a precision welding method that uses a high energy density laser beam as the heat source. Compared with arc welding and electron beam welding technology, the advantages of laser welding are well known: small heat input, fast welding speed and cooling speed, and especially due to the small heat-affected zone, the residual stress is small, etc.^[1]. Therefore, laser welding is widely used in various fields, such as aerospace, automobile production, and shipping.

Laser welding is a process involving rapid heating and cooling. The weld cannot expand or contract freely due to the restrictions on the temperature in the surrounding area. Residual stress and strain will be generated after cooling. In practice, the residual stress of the welded structure usually does not show up immediately. However, it will gradually play a role due to the superposition of stress during the service. Since the welded structure is often subjected to dynamic cyclic loading, when the loading is applied to the welded structure containing residual stress, the loading and the residual stress are combined, which affects the mechanical properties, especially fatigue properties^[2]. Generally, compressive residual stress is beneficial in prolonging the fatigue life and can sometimes be used to improve fatigue strength. However, tensile residual stress plays a detrimental role in fatigue properties, which can cause deformation and cracks. Therefore, research on the welded structure before and after low-cycle fatigue is meaningful.

Laser welding is characterized by highly collimated and concentrated laser beam energy, which makes it challenging to obtain the temperature and strain near the fusion zone during the experiment. In the traditional design process, fatigue properties are usually obtained through a large number of experiments. Not only the experimental period is long, and the cost is high, but many experimental parameters and relationships cannot be directly obtained from

* Corresponding author. afia.kouadri-henni@insa-rennes.fr

the experiment. The development of finite element technology allows us to obtain accurate temperature and stress field results, saving time and money. Abaqus and other numerical methods can be used to investigate the residual stress field as well as the evolution of the residual stress during the laser welding and low-cycle fatigue process.

Recently, the research on residual stress has primarily focused on the effects of process parameters on laser welding residual stress^[3]; the influence of residual stress on microstructure, deformation and mechanical properties^[4-5]; due to the increased use in automotive, fatigue properties of laser-welded dual-phase steel and high-strength low-alloy steel have been a topic of investigation^[6-8].

This paper aims to explore the influencing mechanism of laser welding residual stress on low-cycle fatigue residual stress. First, laser welding residual stress is acquired by different plastic material constitutive models. The obtained residual stress is imported as the predefined stress field for the following simulation. Then, the combined hardening models are employed to evaluate the low-cycle fatigue residual stress. Finally, the effects of laser welding residual stress on low-cycle fatigue residual stress are studied. Furthermore, the simulation results are verified by experimental data.

2. Material

In this paper, DP600 steel is used as the base metal. Usually, DP steel is made by annealing and cooling rapidly and is one kind of AHSS (Advanced High Strength Steel). The microstructure matrix of DP600 steel is ferrite with good plasticity and toughness, and it combines with martensite to improve hardness. The ductility of steel is derived from ferrite, and the strength is derived from martensite. The microstructure of DP600 steel is shown in Fig.1^[9]. DP600 steel has been considered for many applications due to its high tensile strength (654 ± 14 MPa) and low yield strength (310 ± 40 MPa) compared to conventional grades of steel^[10].

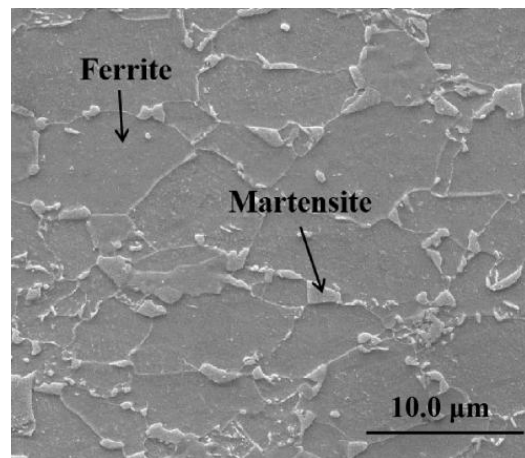


Fig.1. Microstructure of DP600 steel.

3. Simulations

The entire numerical computations consist of thermal and elastic-plastic mechanical and low-cycle fatigue analyses. These two parts are related to the calculation of temperature, laser welding residual stress, and low-cycle fatigue residual stress, respectively. All computations are conducted on the Abaqus platform. This paper focuses on the effects of plastic material constitutive models on the residual stress and the residual stress before and after low-cycle fatigue. The simulation results are further verified through the experiment.

3.1. Finite element model

The specimen geometry used for the finite element model is shown in Fig.2, where the thickness of the base metal is 1.25 mm, with a 0.1 mm gap between the two base metals.

Laser lap welding is used in this paper, with a laser power of 3500 W and a welding speed of 3 m/min. In the low-cycle fatigue simulation, the tensile loading varies a sine function of time with an amplitude of 400 MPa, a stress ratio of 0, and a frequency of 5 Hz.

During the laser welding simulation, temperature-dependent material properties such as thermal conductivity, specific heat, thermal expansion, mass density, Young's modulus and Poisson's ratio are considered. The low-cycle fatigue simulation is carried out at room temperature, the value of material properties at 25 °C is used.

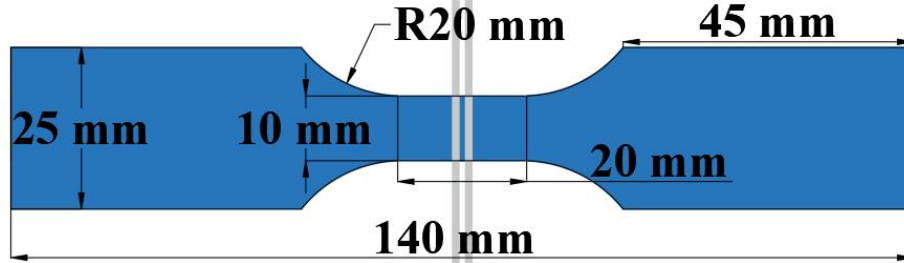


Fig.2. Specimen geometry used for the finite element model.

3.2. Boundary conditions

Boundary conditions in the thermal and mechanical analysis should be defined. The room temperature of 25 °C is considered as the initial condition in both laser welding and low-cycle fatigue simulation. For the boundary conditions in thermal analysis, heat loss due to thermal conduction, convection and radiation is considered. The boundary conditions in the mechanical analysis not only eliminate the rigid body displacements of the model but also do not affect the free deformation of the structure, the same as the experimental conditions.

3.3. Heat source model

Different heat source models have different heat flux distributions and can lead to different heat absorption of materials, which not only affects the accuracy of the laser welding simulation but also affects the distribution of the temperature and residual stress fields. Therefore, selecting the heat source model is very important, as it needs to truly reflect the characteristics of the laser heat source. The conical heat source with Gaussian distribution is used as the heat source model in this paper. The schematic of the conical heat source with Gaussian distribution is shown in Fig.3. This type of heat source helps simulate the welding process with high energy and obtain the weld with concentrated energy and a large aspect ratio, which is closer to the actual situation of laser self-fusion welding^[11]. In Abaqus, the parameters of the heat source model are defined by the DFLUX subroutine.

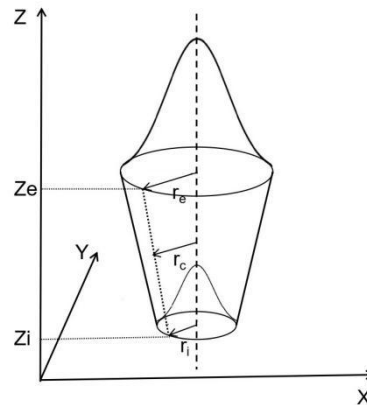


Fig.3. The Conical heat source with Gaussian distribution.

3.4. Plastic material constitutive models

The nominal stress-strain curve can be obtained from the tensile experiment. However, the cross-sectional area and length are nonlinear during the tensile process. The nominal stress-strain curve does not reflect the constitutive relationship in the plastic period. It is necessary to obtain the true stress-strain curve. In order to continue the deformation, external stress must continue to increase when it exceeds the yield strength. This phenomenon is known as strain hardening. Since the external loading applied in the low-cycle fatigue experiment is usually equal to or higher than the yield strength, the material constantly generates strain hardening during the plastic deformation. In summary, the large temperature gradient and applied loading cause plastic deformation and strain hardening, affecting the constitutive relationship and influencing residual stress. It is necessary to establish constitutive models to study the relationship between laser welding and low-cycle fatigue residual stress.

In Abaqus, different plastic material constitutive models can be defined using the UHARD subroutine. In this paper, three strain hardening models are used to describe the plastic deformation ability at a fixed temperature and strain rate^[12] during the laser welding process, namely, the Ludwik Model, the Voce Model, and the Ludwik-Voce Model. Ludwik Model is suitable to describe the strain hardening capacity of martensite combined with a strong hardening effect. And the Voce Model is used to describe material recovery, such as the plastic flow of ferrite. The Ludwik-Voce Model is better for simulating the stress change after the strain value of 0.2. It is a combination of the Ludwik Model and the Voce Model. In the Ludwik-Voce Model, ω is the proportion of martensite that changes in the welding process (0.2 in this paper)^[13]. In equations, the yield strength is shown by a stress factor (σ_0), K , K_1 , K_2 , n , n_1 and n_2 are material parameters. The experimental data come from the stress-plastic strain of the tensile experiment. The fitting curves are shown in Fig.4.

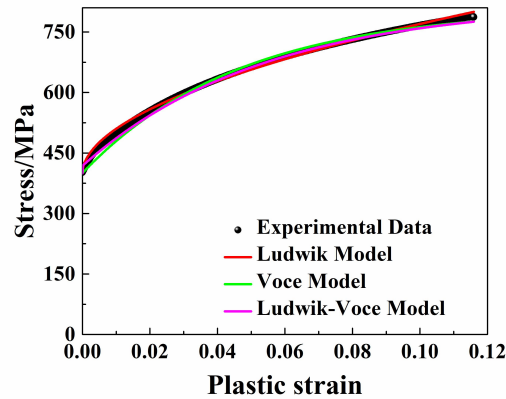


Fig.4. Constitutive models fitting curves.

Table 1. Equations of constitutive models.

Ludwik Model	$\sigma = \sigma_0 + K\varepsilon^n$	(1)
Voce Model	$\sigma = \sigma_0 + K[1 - \exp(-n\varepsilon)]$	(2)
Ludwik-Voce Model	$\sigma = \omega(\sigma_0 + K_1\varepsilon^{n_1}) + (1 - \omega)\{\sigma_0 + K_2[1 - \exp(-n_2\varepsilon)]\}$	(3)

Table 2. Parameters of constitutive models.

	σ_0	K	K_1	K_2	n	n_1	n_2
Ludwik Model	400	1244.24			0.53		
Voce Model	400	409.64			21.55		

Ludwik-Voce Model	400	89.78	506.11	5.02×10^{-11}	18.52
-------------------	-----	-------	--------	------------------------	-------

3.5. Low-cycle fatigue model

Generally, the approach for determining fatigue properties of the welded structure is to establish the S-N curve. This method repeatedly applies periodic loading to the structure until a stable state is obtained. However, this technique is conservative and expensive because many loading cycles may be required before achieving a stable response. Abaqus uses the direct cyclic technique, which combines Fourier series and time integration of the nonlinear material behavior to obtain a stable response directly. The direct cyclic technique effectively solves the problem of time cost due to the need to apply many loading cycles before the stable state is obtained. The basis of this technique is to construct a displacement function $\bar{u}(t)$ to describe the response of the structure at all times t during a load cycle with period T ^[14].

4. Results and discussions

Fig.5 shows the longitudinal and transversal laser welding residual stress curves with three models. All models describe well the residual stress in laser welding of the welded structure. The average value of the longitudinal residual stress is about 180 MPa, the transversal residual stress is about 180 MPa in the center of the weld, and the maximum is about 210 MPa in the heat-affected zone. The residual stress in the heat-affected zone is high because when the heat source acts on a certain point of the weld during laser welding, it will cause the material to expand due to the temperature variation and form an area of compressive stress. The compressive stress is higher than the yield strength at this temperature, so the material undergoes compressive plastic deformation. When the heat source continues moving, the material gradually cools down, and the yield strength increases, thus resulting in high residual stress.

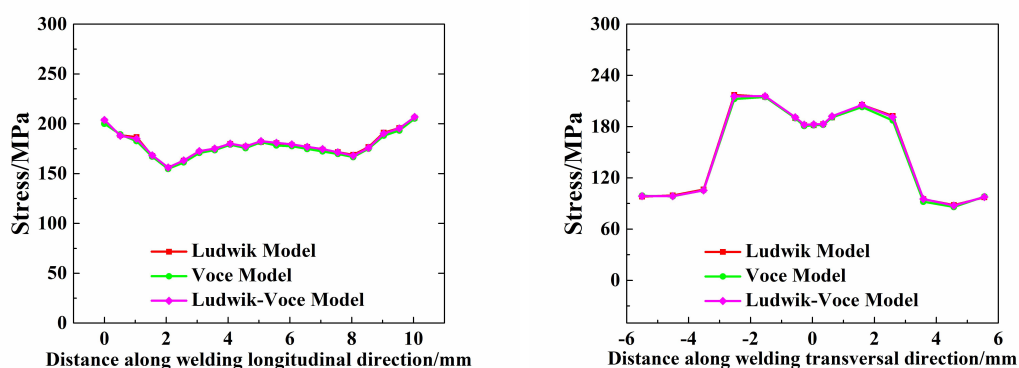


Fig.5. Longitudinal and transversal laser welding residual stress with three models (left) longitudinal residual stress; (right) transversal residual stress.

Fig.6 shows the longitudinal and transversal low-cycle fatigue residual stress curves with three models. It can be seen from Fig.6 that because one end of the welded structure is fixed and the other end is subjected to cyclic loading, the mid-planes of the two base metals are not in a straight line. Under cyclic loading, the welded structure is subjected to torque around the weld. So the distribution of transversal low-cycle fatigue residual stress is asymmetric. The Voce Model is used to describe the plastic flow of the ferrite. Because the ferrite content of the welded structure is larger than the martensite, the Voce Model has a more significant effect on low-cycle fatigue residual stress than the Ludwik Model. The longitudinal residual stress in all models is higher on both sides and lower in the center. In low-cycle fatigue, an important part of the residual stress is the plastic stress generated by plastic deformation during cyclic loading. When only one end of the welded structure is subjected to cyclic loading, the deformation on the two sides is larger than the weld center, so the residual stress is high.

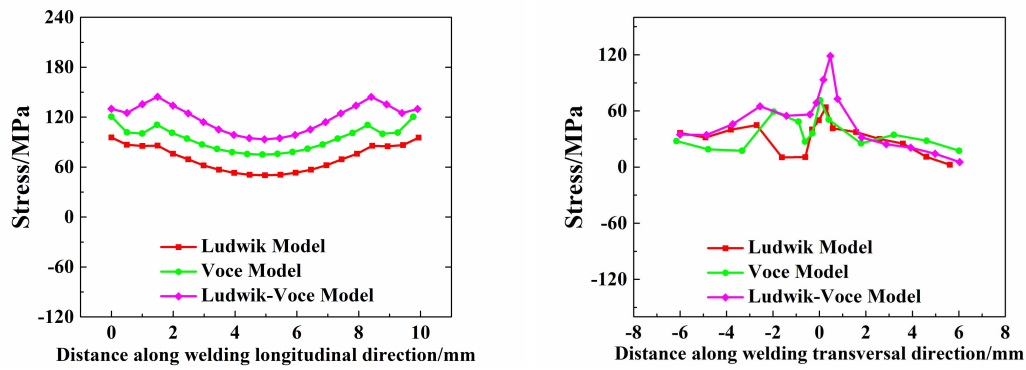


Fig.6. Longitudinal and transversal low-cycle fatigue residual stress curves with three models (left) longitudinal residual stress; (right) transversal residual stress.

Fig.7 shows longitudinal and transversal laser welding and low-cycle fatigue residual stress curves of the Ludwik-Voce Model. The residual stress is redistributed and relaxes after the low-cycle fatigue. When the cyclic loading superposes with the residual stress, the summed stress reaches or is higher than the yield strength, and plastic deformation occurs. In some cases, the summed stress does not reach the yield strength, but it causes local deformation of the welded structure. When the cyclic loading is removed, the welded structure undergoes secondary deformation, so the residual stress is redistributed and relaxes^[15].

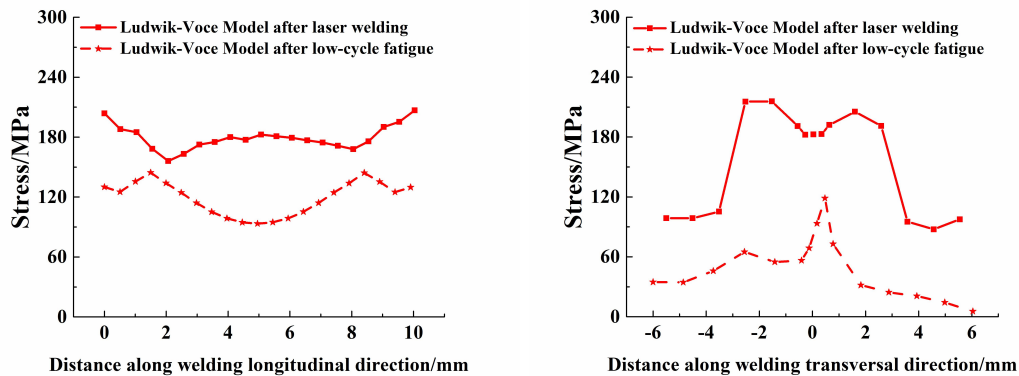


Fig.7. Longitudinal and transversal laser welding and low-cycle fatigue residual stress (left) longitudinal residual stress; (right) transversal residual stress.

Comparing the simulation and experimental results of low-cycle fatigue residual stress, as shown in Fig.8, the trend is the same, but there are still some errors. It is because the fluid flow and phase transformations are neglected in the laser welding simulation, and the laser welding residual stress directly affects the low-cycle fatigue residual stress. Additionally, the initial residual stress present in the base metal is also ignored.

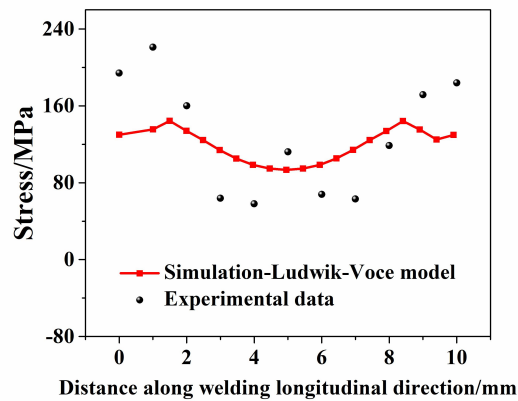


Fig.8. The comparison of simulation and experimental results of low-cycle fatigue residual stress.

5. Conclusions

The following conclusions can be obtained from simulations and experiments for the residual stress after laser welding and low-cycle fatigue of the DP600 steel welded structure:

(1) The large temperature gradient and external loading can cause strain hardening. Constitutive models are used to simulate laser welding residual stress, and combined hardening models are used to simulate low-cycle fatigue residual stress.

(2) The laser welding residual stress reaches the maximum in the heat-affected zone. And the low-cycle fatigue residual stress on both sides of the welded structure is higher than the center along the longitudinal direction of the weld.

(3) Residual stress is redistributed and relaxes after low-cycle fatigue.

(4) Comparing the simulation and experimental results of low-cycle fatigue residual stress, the trend is the same.

Acknowledgements

The work is financially supported by China Scholarship Council (CSC), INSA de Rennes and Laboratory of Digital Sciences of Nantes (LS2N).

References

- [1] Liu W, et al. Numerical modeling and experimental verification of residual stress in autogenous laser welding of high-strength steel. *J. Lasers in Manufacturing and Materials Processing*, 2015, 2(1): 24-42.
- [2] Cho SK, et al. Fatigue strength in laser welding of the lap joint. *J. Finite Elements in analysis and design*, 2004, 40(9-10): 1059-1070.
- [3] Chuan L, et al. Numerical and experimental analysis of residual stresses in full-penetration laser beam welding of Ti6Al4V alloy. *J. Rare metal materials and Engineering*, 2009, 38(8): 1317-1320.
- [4] Rong Y, et al. Laser beam welding of 316L T-joint: microstructure, microhardness, distortion, and residual stress. *J. The International Journal of Advanced Manufacturing Technology*, 2017, 90(5-8): 2263-2270.
- [5] Yilbas BS, et al. Laser welding of AISI 316 steel: microstructural and stress analysis. *J. Journal of Manufacturing Science and Engineering*, 2013, 135(3).
- [6] Westerbaan D, et al. Effects of concavity on tensile and fatigue properties in fibre laser welding of automotive steels. *J. Science and Technology of Welding and Joining*, 2014, 19(1): 60-68.
- [7] Xu W, et al. Tensile and fatigue properties of fiber laser welded high strength low alloy and DP980 dual-phase steel joints. *J. Materials & Design*, 2013, 43: 373-383.
- [8] Parkes D, et al. Microstructure and fatigue properties of fiber laser welded dissimilar joints between high strength low alloy and dual-phase steels. *J. Materials & Design*, 2013, 51: 665-675.
- [9] McCallum B. Characterization of DP600 Steel Subject to Electrohydraulic Forming. *J.* 2014.

- [10] Farabi N, et al. Microstructure and mechanical properties of laser welded DP600 steel joints. *J. Materials Science and Engineering: A*, 2010, 527(4-5): 1215-1222.
- [11] Kik T. Heat source models in numerical simulations of laser welding. *J. Materials*, 2020, 13(11): 2653.
- [12] Chen JJ, et al. Validation of constitutive models for experimental stress-strain relationship of high-strength steel sheets under uniaxial tension[C] *IOP Conference Series: Materials Science and Engineering*. IOP Publishing, 2019, 668(1): 012013.
- [13] Ramazani A, et al. Characterization of microstructure and mechanical properties of resistance spot welded DP600 steel. *J. Metals*, 2015, 5(3): 1704-1716.
- [14] Abaqus I. Abaqus Analysis User's Manual, Volume II: Analysis. J. 2007.
- [15] Benasciutti D, et al. Metal plasticity and fatigue at high temperature. J. 2020.